Statistical Optimization of Culture Conditions and Overproduction of Inulinase using Low Cost, Renewable Feedstocks by a Newly Isolated *Aspergillus sclerotiorum* under Solid-state Fermentation Conditions: Inulin Hydrolysis by Partially Purified Inulinase

Noura El-Ahmady El-Naggar[1]*, E.A. Metwally[2], A.B. El-Tanash[2] and A.A. Sherief[2]

[1]Departement of Bioprocess Development, Genetic Engineering and Biotechnology Research Institute, City for Scientific Research and Technology Applications, Alexandria, Egypt.
[2]Department of Botany, Faculty of Science, Mansoura University, Egypt.

Plate screening assay was used for detection of inulinolytic potentiality produced by some fungal isolates. Among them, strain Hoba2143 was the most active fungal strains able to produce a considerable amount of inulinase. This strain was identified as *Aspergillus sclerotiorum* on the basis of ITS region sequence analysis, together with its phenotypic characteristics. Statistical screening using Plackett-Burman design with 12 run was applied for screening eleven variables on *Aspergillus sclerotiorum* Hoba2143 inulinase production, incubation temperature was the most significant variable at 95% confidence on inulinase yield followed by NH_4 ions, peptone and substrate level, with significant *p*-values of 0.0027, 0.0093, 0.0293 and 0.0309, respectively. These variables were selected for further optimization studies using central composite design to evaluate the effects of four process variables on inulinase production by *Aspergillus sclerotiorum* Hoba2143. The maximum inulinase yield by *A. sclerotiorum* strain Hoba2143 after central composite design was 114.43 Uml^{-1} with a fold of increase 10.69 as compared with the yield after initial survey (10.7 Uml^{-1}) using "Jerusalem artichoke + bagasse" as a substrate for screening inulinolytic potentialities of microorganisms.

Keywords: *Aspergillus sclerotiorum*, inulinase production, solid state fermentation, Plackett-Burman design, central composite design, identification.

Inulin is a widespread poly-fructan accumulated as carbohydrate reserve in the roots and tubers of Jerusalem artichoke, dahlia tubers, chicory, dandelion, burdock and yacon. It consists of linear β- 2, 1-linked polyfructose chains displaying a terminal glucose unit [6]. Inulin has received attention as a relatively inexpensive and abundant material for the production of highly fructose and fructooligosaccharides syrups[53]. Inulinases (β-2, 1-D-fructan fructanohydrolases (EC 3.2.1.7) are one of the most important enzymes in industries; it targets on the β-2, 1 linkage of inulin and hydrolyzes it into fructose [34]. Fructose is widely used in pharmaceutical industry, many foods and beverages instead of sucrose and also can be converted into fuel ethanol by fermentation [7]. Microorganisms are the best sources for commercial production of inulinases mainly due to their easy cultivation and high yields of product. So far, it has been found that microorganisms which can produce high level of inulinases include *Aspergillus tamarii* [37], *Penicillium chrysogenum* ZJ-T2[25], *Staphylococcus* sp. [42], *Streptomyces* sp.[45], and *Pichia guilliermondii* [56].

---

* To whom all correspondence should be addressed.
Tel: (002)01003738444; Fax: (002)03 4593423
E-mail: nouraelahmady@yahoo.com

Molecular identification is widely used for identification of microorganisms, because of the uniformity of inter transcribed spacer (ITS) fragment size in several fungal groups, which makes nucleotide sequencing of ITS fragments necessary to reveal inter specific, and in some cases, also intra specific variation [19].

Traditionally, inulinase is produced by submerged fermentation [16]. In addition, inulinase can also be produced by solid state fermentation (SSF) [6]. Inulinase production by SSF has attracted much attention because of high productivity, simple operation, cost effectiveness and better product recovery [49]. Moreover, the crude fermented products from SSF can be used directly as the enzyme source for biosynthesis and biotransformation [6]. Additionally, these processes are of special economic interest for countries with abundance of biomass and agro-industrial residues, as these can be used as cheap raw materials [4].

Conventional change of one variable-at-a-time approach has been used for optimization process, but it was laborious and time consuming. Statistical optimization can overcome the drawbacks of conventional method and has been extensively used in the optimization of fermentation media. It can result in improved product yields, reduced process variability, closer confirmation of the output response to nominal and target requirements and reduced development time and overall costs [15].

Optimization process by statistical experimental designs is very useful, as it helps in understanding the interactions among the process parameters at different levels and in calculating an optimal level of each parameter for the maximal product yield [36]. Plackett–Burman experimental design (PB) [35] is a very useful tool for picking the significant factors which have strong influence on the response of interest from a list of candidate factors in quite small number of experiments. PB design assumes that there are no interactions between the different media constituents. Response surface methodology (RSM) is a collection of mathematical and statistical techniques useful for modeling and analysis of problems in which a response of interest is influenced by several variables and the objective is to optimize this response [29]. RSM can overcome the drawbacks of conventional method; it can improve product yields, reduce number of experimental runs needed to provide sufficient information for statistically acceptable results, give closer confirmation of the output response to nominal and target requirements and reduce development time and overall costs [15]. Central composite design (CCD) is an experimental design, useful in response surface methodology, for building a second order (quadratic) model for the response variable without needing to use a complete three-level factorial experiment [5].

The present work is an attempt to survey of inulinolytic fungi, one variable-at-a-time approach was investigated. The molecular identification of the most potent inulinase producing strain was reported. The Plackett-Burman experimental design was used for screening the important factors controlling inulinase production under SSF conditions. The factors that had significant effects were optimized using a central composite design (CCD).

MATERIALS AND METHODS

Substrates

Rice straw (RS) as natural waste was bought from local farms in Al-Mansoura, Egypt, cutted into fine particles (about 0.1-0.5 mm), washed and dried at 70°C for 12.0 h. Jerusalem artichoke tubers (J) were washed thoroughly with cold water, sliced and then dried at 100°C for 72h. The dried slices were then milled to a fine powder with a hammer mill. After milling, the resultant powder was used directly as inulin rich source [45].

Isolation and purification of inulinase producing fungi

The fungi were isolated according to Warcup [54]. The soil or rhizosphere sample (25 g) was suspended in 225 ml of sterilized distilled water (1:10; dilution) and subsequently 10 ml of this suspension was added into 990 ml of sterilized distilled water. Petri dishes containing inulin agar medium [31] plus chloranphenicol (100 mg/L) were inoculated with 1.0 ml of the 1:1000 (10^{-3}) diluted soil suspensions. The plates were incubating at 28 ± 2.0ºC and the growth of the colonies was accompanied up to 3.0 days. Fragments of the individual colonies were transferred separately to the same medium for fungal purification or re-

purification and the growth was accompanied for 5.0 days. Similar isolates in their morphological characters on inulin and Potato Dextrose Agar (PDA) plats were collected and grouped for further studies of fungal identification.

Basal medium

The basal medium (free of carbon) used in experiments was contained the following (g/L of acetate buffer; 0.1 M; pH 4.8): peptone, 5.0; $NH_4H_2PO_4$, 8.0; $(NH_4)_2HPO_4$, 4.0; KCl, 0.5; $MgSO_4.7H_2O$, 0.5; and $FeSO_4.7H_2O$, 0.01 [31].

Inoculum preparation

Fungal strains were sub-cultured on modified agar media containing 1.0% inulin as a sole carbon source [31], at 30°C for 5.0 days and maintained at 4°C. Induced slant was mixed with 10 ml sterile basal medium for preparing spore suspension.

Solid state fermentation

Fermentation was carried out in 250 ml Erlenmeyer flasks supplemented with 1g mixed substrate of sugar cane bagasse and Jerusalem artichoke tubers powder with a ratio of 1:1, mixed with 2.0 ml of freshly prepared basal medium in 0.1 M acetate buffer; pH 4.8. The flasks were covered with hydrophobic cotton and autoclaved at 121°C at 15 lbs for 20 min. after cooling, each flask was inoculated under aseptic conditions and distributed carefully with 2.0 ml spore suspension previously prepared (The final moisture content was 80%) and incubated for 5.0 days at 30°C under static conditions.

Extraction of inulinase

The fermented substrates were mixed and homogenized well with 50 ml of 0.1M acetate buffer (pH 4.8); the mixture was shaken thoroughly on a rotary shaker (150 rpm) at room temperature (20±2æ%C) for 60 min. The mixtures were filtered through muslin cloth; then centrifuged at 5000 *g* for 10 min. After centrifugation, the supernatant was collected and stored in a deepfreeze (-20°C) until it was used as crude inulinase [6].

Inulinase assay

The inulinase activity was determined by measuring the reducing sugars released by the hydrolysis of inulin according to Somogyi [50] method. The assay mixture for inulinase contained 0.1 ml of crude enzyme and 0.1 ml of 0.1 % (w/v) inulin (freshly prepared in 0.1 M sodium acetate buffer; pH 4.8). The reaction mixture was incubated at 40°C for 30 min; then, liberated reducing sugars were determined at 700 nm using Spectro UV–VIS RS spectrophotometer.

The absorbance was related to the concentration of fructose according to the standard calibration curve. One unit (U) of inulinase was defined as the amount of enzyme that released one µmole of fructose per minute from inulin at 40°C and other assay conditions.

Estimation of soluble protein

The soluble protein concentration was determined by the method of Bradford [3]. 0.5ml of the supernatant was mixed by 2.5 ml commasie brilliant blue reagent (G250) and the optical density was measured against blank at 595 nm after 2 min and before 1 hr using Spectro UV-VIS RS spectrophotometer. The µg of protein was estimated using standard curve of bovine serum albumin (BSA).

Fungal identification

Fungal strains were sent as pure slants to Regional Center for Mycology and Biotechnology (RCMB), Al-Azhar University, Nasr City, Cairo, Egypt for identification. All isolates were grown on Czapek Agar (PDA) medium, observing its macroscopic characteristics (colour, texture appearance and diameter of the colonies) and microscopic (microstructures), according to Domsch *et al.* [11]; Samson [39] for the genus *Aspergillus*

Scanning electron microscopy

For scanning electron microscopy (SEM), the gold-coated specimen was examined at different magnifications with Analytical Scanning Electron Microscope (JSM-6510 LV) at Electron Microscope unit, Mansoura University, Egypt

Molecular identification

Molecular identification was performed by Macrogen Korea Company Gasan-dong, Geumchen-gu, Seoul, Korea (http://www.macrogen.com).

The genomic DNA was isolated by transferring fungal mycelium with a sterilized toothpick, suspended in 0.5 ml of sterilized saline in a 1.5 ml centrifuge tube and centrifuged at 10,000 rpm for 10 min. Then the supernatant was discarded and the pellet was re suspended in 0.5 ml of InstaGene Matrix (Bio-Rad, USA). Incubated at 56°C for 30 min and then heated 100°C for 10 min. After heating, supernatant can be use for PCR.

The amplification of ITS1-5.8S-ITS2 regions of rDNA was performed in a total volume of 100 µl, which contained 1 µl DNA, 10 µl of 250 mM deoxyribonucleotide 5'-triphosphate (dNTP's); 10 µl PCR buffer, 3.5 µl 25 mM MgCl2 and 0.5 µl Taq polymerase, 4 µl of 10 pmol (each) forward primer ITS1 (3'-TCCGTAGGTGAACCTGCGG-5') and reverse primer ITS4 (5'-TCCTCCGCTTA TTGATATGC -3') and water was added up to 100 µl. The PCR-apparatus was programmed as follows: 5 min denaturation at 94°C, followed by 35 amplification cycles of 1 min at 94°C, 1 min of annealing at 55°C, and 2 min of extension at 72°C, followed by a 10 min final extension at 72°C. Unincorporated PCR primers and dNTPs were removed from PCR products by using Montage PCR Clean up kit (Millipore). The PCR reaction mixture was then analyzed via 1% (w/v) agarose gel electrophoresis, and the remaining mixture was purified using QIA quick PCR purification reagents (Qiagen, USA). The purified PCR products were sequenced. Sequencing reactions were performed in a MJ Research PTC-225 Peltier Thermal Cycler using a ABI PRISM® BigDyeTM Terminator Cycle Sequencing Kits with AmpliTaq-DNA polymerase (FS enzyme) (Applied Biosystems), following the protocols supplied by the manufacturer. Single-pass sequencing was performed on each template using the last mentioned PCR-primers. The fluorescent-labeled fragments were purified from the unincorporated terminators with an ethanol precipitation protocol. The samples were resuspended in distilled water and sequencing products were resolved on an Applied Biosystems model 3730XL automated DNA sequencing system (Applied BioSystems, USA). The sequencing product was deposited in the GenBank database under accession number KC020123 for *Aspergillus sclerotiorum* strain Hoba2143.

Phylogenetic analysis and identification of fungal strain

The obtained sequence was analyzed using the basic local alignment search tool (BLAST) at NCBI database (http://blast.ncbi.nlm.nih.gov). For comparison with currently available sequences, 57 sequences were retrieved with over 98% similarities belonging to 57 different genera and multiple alignments were performed. Phylogenetic tree obtained by neighbor-joining analysis [38] of 18S ribosomal RNA gene

(partial), internal transcribed spacer 1, 5.8 S ribosomal RNA gene, internal transcribed spacer 2 and 28 S ribosomal RNA gene (partial), showing the position of *A. sclerotiorum* strain Hoba2143 within the genus *Aspergillus*. The phylogenetic analysis was accomplished by using the Mega 4 software program [51].

Rapid plate assay of the inulinolytic potentiality of the most active strain

The inulinolytic potentiality of *Aspergillus sclerotiorum* strain Hoba2143 was detected by spot inoculation on inulin agar plates. It was then flooded with 1% Lugol's iodine and examined for a zone of clearance around the colony which indicated the presence of the enzyme inulinase [25].

Statistical optimization of inulinase production by *A. sclerotiorum*

A prior knowledge with understanding of the related bioprocesses is necessary for a realistic modeling approach. J+RS in ratio (1:1) as a carbon source and incubation period of four days were selected for optimization studies of inulinase production by *A. sclerotiorum* Hoba 2143.

Plackett–Burman experimental design

The Plackett–Burman design (PB) is an efficient technique for the optimization of medium component. PB is very useful for picking the most important factors from a list of candidate factors. At this early problem-solving stage, the methodology assumes that important main effects will be much larger than two-factor interactions, so we were willing to confound the main effects. The technique was used to identify the most important independent variables, to verify if the investigated levels were in adequate range and to select them to realize another fractional design or a complete factorial design [35]. The results of PB experimental design were fitted by the first-order model as follows:

$$Y = \beta_0 + \Sigma \; \beta_i X_i \quad (i=1, 2, \ldots\ldots k) \qquad \text{Eq. (1)}$$

Where; Y is the estimated target function; β_0 is the model intercept and âi is the regression coefficient and X_i is the coded independent factor and k is the number of studied factor. Each variable was defined at two levels, namely high and low level that was coded by (+1) and (–1). The studied variables in our experimental design were as the

following; peptone (A), $NaNO_3$ (B), NH_4 mixture contain $NH_4H_2PO_4 + (NH_4)_2HPO_4$; in ratio 2:1 (C), KCL (D), $MgSO_4$ (E), $FeSO_4$ (F), $CaCl_2$ (G), initial pH (H), inoculum size (I), substrate level (K) and incubating temperature (L). The statistical software package "Design Expert 7.0.0" is used to analyze the experimental data.

Central composite design (CCD)

The central composite design (CCD) was used to further investigate the optimal level points of key factors obtained from PB design in the production of inulinase as response. The experimental variables were coded according to the following equation:

$$X_i = (x_i - x_0)/\Delta x_i \quad (i = 1, 2, \ldots, k)$$

Where; X_i was the coded value of an independent variable, x_i was the real value of an independent variable, x_0 was the real value of an independent variable at the center point, and x_i was the value of step change, and k; number of variables =4

The most significant factors obtained by PB design including; incubating temperatures (X_1), NH_4 mixture (X_2), substrate level (X_3), and peptone (X_4) were selected; while, insignificant ones were eliminated in order to obtain a smaller, manageable set of factors. The four independent variables were studied at five different levels; sets of 30 experiments are carried out. The statistical software package "Design Expert 7.0" was used to analyze the experimental data. All variables were taken at a central coded value of zero. The average maximum inulinase activity was taken as the response (Yp). A multiple regression analysis of the data was carried out for obtaining an empirical model that relates the response measured to the independent variables. A second-order polynomial equation is:-

$$Y_p = \beta_0 + \sum_{i=1}^{4} \beta_i x_i + \sum_{i=1}^{4} \beta_{ii} x_i^2 + \sum_{i,j=1}^{4} \beta_{ij} x_i x_j$$

- Eq. (2)

Where Y_p is the measured response, β_0 is the intercept term, β_i are linear coefficients, β_{ii} are quadratic coefficient, β_{ij} is interaction coefficient, and X_i and X_j are coded independent variables. The optimal values of the critical variables are obtained by analyzing 3D plots. The statistical analysis of the model is represented in the form of analysis of variance (ANOVA).

Determination of hydrolysis products

The hydrolysis products of inulin by *Aspergillus sclerotiorum* Hoba2143 purified inulinase were determined by thin layer chromatography (TLC) using 20x20 cm silica gel 60 F254 plate (Merck, TLC aluminium sheets). 0.1 ml of enzyme mixed with 0.1 ml inulin (0.3 0%; pH; 4.8) was incubated at optimum temperature for interval times (5, 10, 15 and 30 min). After incubation, the reactions were stopped by adding 0.3 ml absolute alcohol (95%); then, the liberated free sugars were examined through descending plate. Control (inulin mixed with inactive inulinase) and authentic samples of sucrose, glucose, and fructose were also spotted and air dried. The plate was placed in a glass tank filled with develop solution (35 acetic acid: 30 chloroform: 5 water) and stored for 4.0 h at room temperature. On removed and air-dried plate, carbohydrates were detected by staining with aniline-diphenylamine reagent. This reagent was prepared by mixing a solution of 1 ml of aniline and 1 g of diphenylamine in 100 ml acetone, with 10 ml 85% phosphoric acid; the latter component was added just prior to use. The plate was sprayed with the staining reagent and color developed after heating for 15 min. at 120 °C. Using this procedure fructose and fructose oligomers are visualized as brown spots, glucose as a blue spot and sucrose as a dark green spot. The colors are clearly visible for up to 6 h [1].

RESULTS AND DISCUSSION

Screening of fungal strains for their inulinolytic potentialities by solid state fermentation technique.

This experiment was done in order to screen potential inulinase producers, detect their abilities for hard waste degradation. The results indicated that *Aspergillus sclerotiorum* (534.78±1.37 Ugds[-1]), *Emericella nidulans* (495.73±3.85 Ugds[-1]), and *Aspergillus aculeatus* (444.37±2.37 Ugds[-1]) were generally the most active fungal strains able to produce a considerable amount of inulinase. Based on the specific activities of the screened inulinolytic fungal species, *Aspergillus sclerotiorum* attained the highest specific activity of 338.47(U/mg protein) and was selected to be the most active species used for further investigations.
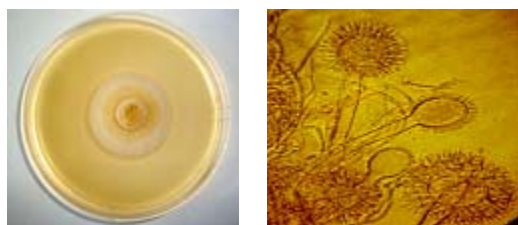
Macroscopic and microscopic examination of the most active strain

Colonies reaching 3-4cm diameter in 7 days at 28°C, on Czapek, yellow to buff with light yellow conidia, mycelium white, not dense, zonate, reverse brown. Radiate conidial heads, presence of upright conidiophores (9.0 μm in diameter) that terminated in globose (26.0 μm) vesicle, with two layers of first sterigmata (7.9 X 3.0 μm) and second sterigmata (5.5 X 2.2 μm), with spherical conidiospores (3.0 μm) on it (Fig. 1).

Scanning electron microscopy (SEM) with high resolution and great depth of focus has been used to show the fine features of surface ornamentation of fungi, and with this technique we could obtain the interesting results about the surface structures of the selected fungi. The three dimensional SEM micrographs were excellent tools that documented the light microscopic identification of *A. sclerotiorum*. The SEM micrographs in Fig. 2 showed upright, rough walled conidiophores, bearing radiate conidial heads with spherical vesicles, covered with biseriate phialides carrying chains of spherical conidia with smooth to finely roughened walls that are identical to that of *A. sclerotiorum*.

**Molecular identification of the most active inulinase producing fungal strain**

The ITS region of the most active inulinolytic strain was amplified, sequenced and deposited in the GenBank database under accession number KC020123. Amplification with primers ITS1 and ITS4 resulted in approximately 562 bp of fragment. The obtained sequence was compared with those in the NCBI Nucleotide Sequence Database by using the BLAST algorithm at the website http://www.ncbi.nlm.nih.gov/BLAST. A comparative analysis by software

package MEGA4 version 2.1 demonstrated that ITS region sequence from the parental strain had a significant identity to a number of Aspergilli section; the comparison of the parental strain sequence with sequences of the reference species of *Aspergillus* contained in genomic database banks exhibited a similarity of 98% with *Aspergillus sclerotiorum* CCF: 3431 (FR733827.1).

The phylogenetic tree obtained by applying the neighbor-joining method is illustrated in Fig. 3. The topology of the phylogenetic tree was evaluated by using the bootstrap resampling method of Felsenstein [14] with 1000 replicates. From the Fig. 3, it is obvious that the isolate is closely similar to *A. sclerotiorum* CCF: 3431 (Gene Bank accession no. FR733827.1) followed by *A. ochraceus* DBOF-107 (JQ724468.1). Accordingly, the fungus strain was identified as *A. sclerotiorum* Hoba 2143. According to the analysis of ITS region sequence, together with its phenotypic and characteristics, the parental strain was identified

Fig. 1. Macroscopic and microscopic characteristics of *A. sclerotiorum*. A) Colonies B) Radiate conidial heads.
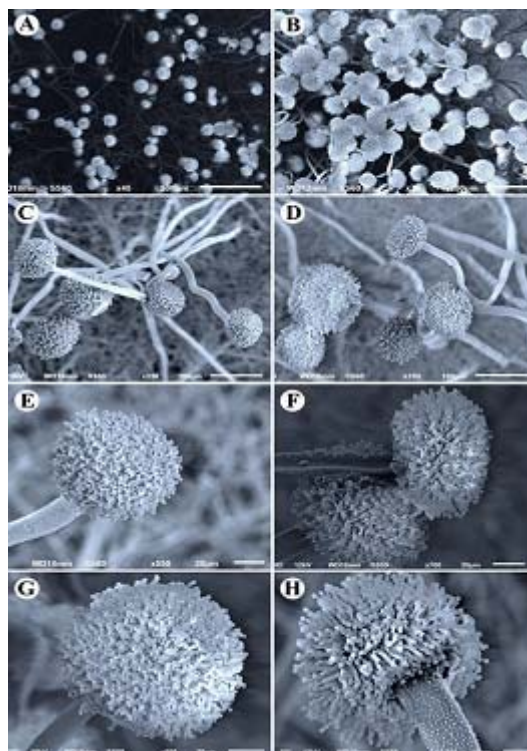

Fig. 2. Scanning electron micrographs of A. sclerotiorum ; A, B, C, D, E, F, G and H at different magnifications 45x, 75x, 230x, 250x, 550x, 700x, 800x and 1200x respectively.

as *Aspergillus sclerotiorum* and designated as *Aspergillus sclerotiorum* strain Hoba2143. Molecular identification techniques exhibit high sensitivity and specificity for identifying microorganisms and can be used for classifying microbial strains at diverse hierarchical taxonomic levels. These techniques, which based on the PCR amplification of genes coding for rRNAs and sequence comparison, offer a new rapid tool for identification of filamentous fungi using two specific PCR primers sets. The sequence is exemplified in the detailed description of the 18S rRNA gene, through the internal transcribed spacer 1; 5.8S rRNA gene (ITS1), ITS2, and into the 28S rRNA gene, each species has a unique nucleotide sequence through this stretch of genes [43].

Rapid plate assay of the inulinolytic potentiality of the most active inulinase strain

Plate screening assay is commonly used for detection of extracellular hydrolytic enzymes produced by microorganisms. The inulinolytic potentiality of *Aspergillus sclerotiorum* strain
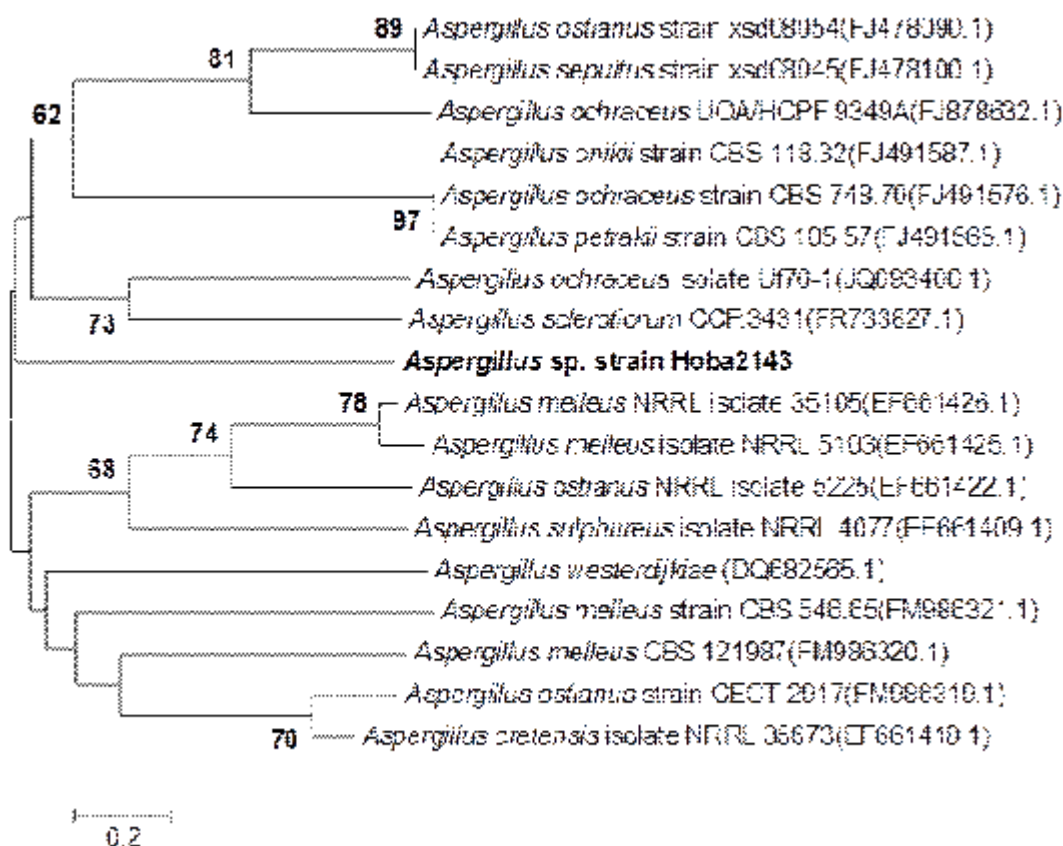
Fig. 3. Phylogenetic tree obtained by neighbor-joining analysis of 18S ribosomal RNA gene (partial), internal transcribed spacer 1, 5.8S ribosomal RNA gene, internal transcribed spacer 2 and 28S ribosomal RNA gene (partial), showing the position of *Aspergillus* sp. strain Hoba2143 within the genus *Aspergillus*. Only bootstrap values above 50 %, expressed as percentages of 1000 replications, are shown at the branch points. GenBank sequence accession numbers are indicated in parentheses after the strain names. Phylogenetic analysis was conducted in MEGA4. Bar, 0.2 substitution per nucleotide position.

Hoba2143 on inulin agar plates was detected by the formation of a clear hydrolytic zone surrounding the fungal colony (Fig. 4) after incubation and staining with Lugol's iodine solution. The ratio of the hydrolytic zone diameter to the colony diameter (H/C) was estimated to be 1.14 cm.

Statistical screening of fermentation process variables for inulinase production by *A. sclerotiorum* strain Hoba2143 using Plackett-Burman design

Plackett-Burman (PB) design was used to determine which variables significantly affect inulinase production by *A. sclerotiorum* strain Hoba2143, then the significant factors were chosen for further studies and insignificant ones were eliminated in order to obtain a smaller, manageable set of factors. One of the interesting properties of PB designs is that all main effects are estimated with the same precision. The influence of eleven medium factors and conditions namely peptone, $NaNO_3$, NH_4 mixture, KCl, $MgSO_4$, $FeSO_4$, $CaCl_2$, initial pH, inoculum size, substrate level and incubating temperature in the production of inulinase by *A. sclerotiorum* Hoba2143 through solid state fermentation was investigated in 12 runs using PB design. Selected variables with low level ("1) and high level (+1) are illustrated in Table 1. In the experimental design, each row represents an experiment and each column represents an independent variable. The signs + and - represent the two different levels (higher and lower) of the independent variable under investigation. The PB design for the 11 selected variables and the corresponding response for inulinase production are shown in Table 1. The inulinase yield varied markedly with the variables tested in range of 0.45 to 84.73 Uml^{-1} in the 12 trials, this variation reflects the importance of medium optimization to attain higher productivity.

The lowest value of inulinase yield (0.45 Uml^{-1}) was obtained in run no. 4 when minimal levels of $NaNO_3$, NH_4 mixture, KCl, $FeSO_4$, $CaCl_2$ and inoculum size and maximal levels of peptone, $MgSO_4$, $CaCl_2$, initial pH, substrate level and incubating temperature were used, while the highest value of inulinase yield (84.73 Uml^{-1}) was obtained in run no.7 when peptone, $NaNO_3$, NH_4 mixture, $CaCl_2$, inoculum size and substrate level were adjusted to the highest levels and KCl, $MgSO_4$, $FeSO_4$, initial pH and incubating temperature were adjusted to the lowest levels. These results suggest that some variables significantly affect the inulinase activity while others not.

Statistical analysis of Plackett-Burman design for inulinase production by *A. sclerotiorum* strain Hoba2143

The experimental design along with the responses of different experimental trials is shown in Table 2. Statistical analysis of the response (inulinase production) was performed and estimated effect is represented in Table 3. The data revealed that, initial pH (H) and $NaNO_3$ (B) are two insignificant variables with lower effects (1.79 and -2.88, respectively) and lower percent of contribution (0.09 and 0.24, respectively). Lower % of contribution indicated higher *p*-value. Thus instead of starting with the maximum model effects, backward regression at alpha 0.15 was applied to remove/or eliminate the small effects of pH (H) and $NaNO_3$ (B). Then, the model fitted for the test of

Table 1. The levels of the screened independent variables used for inulinase production during SSF under Plackett–Burman design

Variable code	Name	Unit	Low actual(-1)	High actual(1)
A	Peptone	%	0.2	0.7
B	$NaNO_3$	%	0.2	0.7
C	NH_4 mixture	%	0.6	1.8
D	KCL	%	0.03	0.07
E	$MgSO_4$	%	0.03	0.07
F	$FeSO_4$	%	0	0.002
G	$CaCl_2$	%	0.03	0.07
H	Initial pH	Degree	4.2	5.4
I	Inoculum size	ml spores suspension 1g dry substrate^{-1}	0.5	2
K	Substrate level	g 250 ml flask^{-1}	0.7	1.3
L	Temperature	°C	25	35

significance. Actually, the removal procedure ends when the model was at significant level.

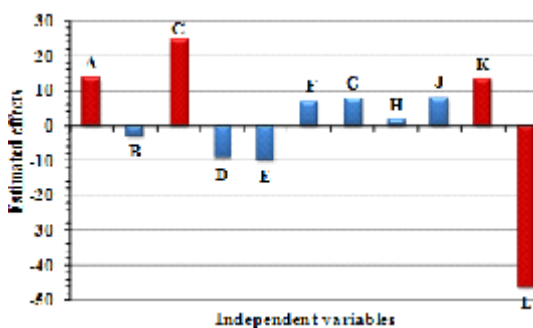Pareto chart allows detecting the order and significant effects of variables affecting inulinase production in PB experimental design. It displays the absolute values of the effects, and draws a reference line on the chart. Any effect that extends past this reference line is potentially important. Pareto chart in design expert version 7.0 reproduce the relation between *t*-value (effect) vs. ranks. Pareto chart (Fig. 5) showed that incubating temperature (L) was the most significant variable affecting inulinase production at 95% confidence followed by mixture of NH_4 (C), peptone (A) and substrate level (K), while other variables $MgSO_4$ (E), KCl (D), inoculum size (J), $CaCl_2$ (G) and $FeSO_4$ (F) are not significant. Also, it was clear that the significant variables of mixture of NH_4, peptone and substrate level had positive effects on inulinase production while, incubating temperature has negative effect.

The analysis of variance (ANOVA) of the experimental design (after removal of lower effects variable) was calculated, and the significant levels of each variable were determined by Fisher's *F*-test and summarized in Table 4. The ANOVA of the PB design demonstrated that the model was highly significant as was evident from the Fisher's *F*-test with a very low probability value [(*P* model>*F)* =0.0148]. The model *F*-value of 67.17 implies the model is significant. There is only 1.48% chance that a "Model *F*-value" this large could occur due to noise. Also factors evidencing *P*-values of less than 0.05 were considered to have significant effects on the response (inulinase production).

In this connection the analysis showed that, incubation temperature (L) with a probability value of 0.0027 was determined to be the most significant factor affecting inulinase production by *A. sclerotiorum* strain Hoba2143 followed by NH_4 mixture (C), peptone (A) and substrate level (K) with probability values of 0.0093, 0.0293 and 0.0309 respectively, the lower probability values
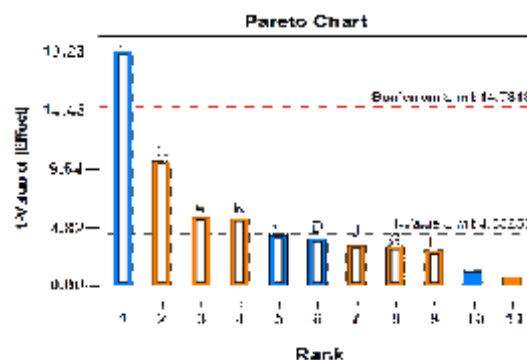

Fig. 4. Inulin agar plates stained with Lugo's iodine solution before (plates to the left) and after (plates to the right) incubation period of *A. sclerotiorum* strain Hoba2143, front (A) and rear (B) view.

Fig. 5. (A) Effect of independent variables on inulinase production by *A. sclerotiorum* strain Hoba2143 based on Plackett-Burman design, (B) Pareto chart illustrates the order and significance of the variables affecting inulinase production by *A. sclerotiorum* strain Hoba2143 (the blue colors represent negative effects and the orange color represent positive effects).

indicate the more significant factors affecting inulinase production. Among the four significant variables screened, only incubation temperature exerted a negative effect, whereas the other variables NH_4 mixture, peptone and substrate level exerted positive effects on inulinase production. On the other hand, all other model variables were determined to be insignificant factors.

The goodness of fit of the model was checked by the determination coefficient (R^2). The R^2 values provide a measure of how much variability in the observed response values can be explained by the experimental factors. The R^2 value is always between 0 and 1. The closer the R^2 value is to 1, the stronger the model is and the better it predicts the response. In our study, the value of the determination coefficient ($R^2 = 0.9967$) indicated that 99.67% of the variability in the response could be explained by the model and only 0.33% of the total variations are not explained by the model. In addition, the value of the adjusted determination coefficient (Adj. $R^2 = 0.9819$) was also very high to advocate for a high significance of the model (Table 4). The higher the Adj. R^2 the more accuracy of the relationships between the studied variables and inulinase production. At the same time the

Table 2. Plackett-Burman experimental design for evaluating factors influencing inulinase production through solid state fermentation by *A. sclerotiorum* strain Hoba2143

| Run No. | Coded levels of independent variables | | | | | | | | | | | Inulinase yield (Uml^{-1}) |
	A	B	C	D	E	F	G	H	J	K	L	
1	-1	+1	+1	+1	-1	-1	-1	+1	-1	+1	+1	1.54
2	+1	-1	+1	+1	-1	+1	+1	+1	-1	-1	-1	65.71
3	+1	+1	-1	+1	+1	+1	-1	-1	-1	+1	-1	31.88
4	+1	+1	+1	-1	-1	-1	+1	-1	+1	+1	-1	84.73
5	-1	+1	-1	+1	+1	-1	+1	+1	+1	-1	-1	15.54
6	-1	-1	+1	-1	+1	+1	-1	+1	+1	+1	-1	64.91
7	+1	-1	-1	-1	+1	-1	+1	+1	-1	+1	+1	0.45
8	+1	+1	-1	-1	-1	+1	-1	+1	+1	-1	+1	1.53
9	+1	-1	+1	+1	+1	-1	-1	-1	+1	-1	+1	1.07
10	-1	-1	-1	-1	-1	-1	-1	-1	-1	-1	-1	20.09
11	-1	-1	-1	+1	-1	+1	+1	-1	+1	+1	+1	0.71
12	-1	+1	+1	-1	+1	+1	+1	-1	-1	-1	+1	0.47

Signs (+) and (-) represent the higher and lower levels of the independent variable.

Table 3. Estimated effect, sum of squares and % of contribution for inulinase production by *A. sclerotiorum* strain Hoba2143 using PB design

Term	Estimated effect	Sum of Squares	% Contribution
A- Peptone	13.68	561.80	5.38
B- NaNO$_3$	-2.88	24.85	0.24
C- NH$_4$ mixture	24.71	1831.51	17.55
D- KCl	-9.29	258.84	2.48
E- MgSO$_4$	-10.00	300.00	2.87
F- FeSO$_4$	6.97	145.63	1.40
G- CaCl$_2$	7.77	181.02	1.73
H- Initial pH	1.79	9.57	0.09
J- Inoculum size	8.06	194.87	1.87
K- Substrate level	13.30	530.72	5.08
L- Incubation temperature	-46.18	6398.21	61.30
Lenth's ME	37.46		
Lenth's SME	80.24		

predicted-R^2 value of 0.8813 for the inulinase production by *A. sclerotiorum* strain Hoba2143 was in a reasonable agreement with the Adjusted-R^2 of 0.9819 which indicated that the model is good. Predicted-R^2 indicates how well the model predicts responses for new observations, thus our results revealed that the inulinase production through PB design could be predicted with 88.13% accuracy. The adequate precision value of the present model was 23.49 and this also suggests that the model can be used to navigate the design space. The 'adequate precision value' is an index of the signal-to-noise ratio, and values of higher than 4 are essential prerequisites for a model to be a good fit. The model showed standard deviation, mean, coefficient of variation and PRESS value of 4.148, 24.052, 17.246 and 1238.92 respectively. ANOVA analysis confirmed a satisfactory adjustment of the model to the experimental data.

To approach the neighborhood of the optimum response, the coefficients of regression equation were calculated using design expert version 0.7 and the data Table 5 was fitted to a first order polynomial equation. By neglecting the insignificant terms the following equation was obtained.

$$Y_{(Inulinase\ yield)} = +24.05 +6.84A +12.35C +6.65K - 23.09L \qquad Eq.\ (3)$$

Where Y is the response (inulinase yield), and A, C, K, and L are peptone, NH_4 mixture, substrate level and incubation temperature; respectively. The coefficient of each variable represents the effect extent of these variables on inulinase yield. Moreover, Equation (3) showed that the coefficients of peptone, NH_4 mixture and substrate level were positive (6.84, 12.35 and 6.65 respectively); while the coefficient of incubation temperature was negative (-23.9), which means that the increase in the concentrations of peptone, NH_4 mixture, substrate level and decrease in incubation temperature could exert positive effect on inulinase yield.

On the basis of *P* values (Table 4), peptone, NH_4 mixture, substrate level and incubation temperature were chosen for further optimization using central composite design (CCD), since these factors had the most significant effects on inulinase production.

Nitrogen source is one of the most important factors that affect the growth and metabolites of microorganisms, as it included in the synthesis of amino acids, enzymes, nucleotides, vitamins and some carbohydrates, thus variation in the nitrogen source can affect the metabolic processes of the cell significantly. The microbial production of enzymes that can show

Table 4. Regression statistics and analysis of variance (ANOVA) for the experimental results of Plackett-Burman design used for inulinase production by *A. sclerotiorum* strain Hoba2143

Source	Sum of Squares	*df*	Mean Square	*F*-value	*P*-value *Prob >F*
Model	10402.58	9	1155.84	67.17	0.0148*
A- Peptone	561.80	1	561.80	32.65	0.0293*
C- NH_4 mixture	1831.51	1	1831.51	106.44	0.0093*
D- KCl	258.84	1	258.84	15.04	0.0605
E- $MgSO_4$	300.00	1	300.00	17.43	0.0529
F- $FeSO_4$	145.63	1	145.63	8.46	0.1006
G- $CaCl_2$	181.02	1	181.02	10.52	0.0833
J- Inoculum size	194.87	1	194.87	11.32	0.0781
K- Substrate level	530.72	1	530.72	30.84	0.0309*
L- Incubation temperature	6398.21	1	6398.21	371.83	0.0027*
Residual	34.41	2	17.21		
Cor Total	10437.00	11			
Std. Dev.	4.148166	R-Squared	0.996703		
Mean	24.05208	Adj R-Squared	0.981865		
C.V. %	17.2466	Pred R-Squared	0.881295		
PRESS	1238.924	Adeq Precision	23.4897		

* Significant values, *df* : Degree of freedom, *F*: Fishers's function, *P* : Level of significance C.V: Coefficient of variation

interesting biochemical properties for biotechnological application depends primarily on the nature of the organism as well as on culture medium composition [2], so the proper application of a convenient nitrogen source is very important for optimal enzymes production [27].

In this connection our results revealed that, both organic (peptone) and inorganic (ammonium phosphate) nitrogen sources have positive effects on inulinase production by *Aspergillus sclerotiorum* Hoba2143 where, peptone shown a maximum inulinase production (114.43 U/ml) at 0.64% (w/v) peptone concentration, the stimulatory effect of peptone on inulinase production has been reported by Singh et al. [48]. Kaur et al. [22] recorded a maximum inulinase production by *Aspergillus fumigatus* at 34°C on a medium containing combination of peptone and $NaNO_3$, also the work of Li et al. [26] revealed a maximum inulinase activity (14.6 ± 0.4 U/ml) at 1% (w/v) peptone concentration. In other studies it was reported that each fungal species has a preference for a specific organic or inorganic nitrogen source for maximum inulinase production [23]. *Penicillium* sp.TN-88 was reported to have high inulinase activity with yeast extract as the organic nitrogen source [52]. Also Jing et al. [20] observed maximum inulinase production (21.54 U/ml) by *Aspergillus ficuum* when peptone is replaced by yeast extract. For *Penicillium citrinum* AR-IN2, El-Hersh et al. [12] found that, corn steep liquor (CSL) is a potent inducer for inulinase production (35.6U/ml).

On the other hand, our results also revealed that, the inorganic nitrogen source (ammonium phosphate mixture) is a very potent stimulator for inulinase production, where the maximum inulinase activity (114.43 U/ml) was recorded at 1.54% (w/v) NH_4 mixture ($NH_4H_2PO_4$ + $(NH_4)_2HPO_4$), further increasing of NH_4 mixture concentration decreased inulinase activity, the same results were recorded by Sanal et al. [40], ammonium phosphate was the best nitrogen source for inulinase production from *Alternaria alternata*. The work of Derycke and Vandamme [9]; Jing et al. [20] and Xiong et al. [55] showed that the addition of ammonium salts to the medium resulted in higher production of inulinase in *Aspergillus niger*, *A. ficuum* (0.5% $NH_4H_2PO_4$ gave the highest level of inulinase activity) and *Kluyveromyces* S120 respectively. Also the study of Kumar et al.[24] on *Aspergillus niger* AUP19 revealed that $NH_4H_2PO_4$ showed maximum inulinase production (87 U/ ml) followed by $(NH_4)_2HPO_4$ (74 U/ ml).

In contrast to our results, Singh and Singh [47] found that the presence of ammonium salts in the production medium usually inhibit the growth and synthesis of inulinase, this may be attributed to the acidic conditions resulted due to the utilization of ammonium ions and liberation of acids into the medium. In this regard, Singh et al. [48] reported the inhibitory effect of ammonium salts on inulinase production from *K. fragilis*. Dinarvand et al. [10] recorded that inulinase production in the culture medium of *Aspergillus niger* ATCC 20611 supplemented with 0.5 and 1% of $NH_4H_2PO_4$

Table 5. Regression coefficients of Plackett-Burman design variables
for inulinase production by *A. sclerotiorum* strain Hoba2143

Factor	Coefficient estimate	df	Standard error	95% CI Low	95% CI High
Intercept	24.052	1	1.20	18.900	29.204
A-Peptone	6.842	1	1.20	1.690	11.995
C-NH_4 mixture	12.354	1	1.20	7.202	17.506
D-KCl	-4.644	1	1.20	-9.797	0.508
E-$MgSO_4$	-5.000	1	1.20	-10.152	0.152
F-$FeSO_4$	3.484	1	1.20	-1.669	8.636
G-$CaCl_2$	3.884	1	1.20	-1.268	9.036
J-Inoculum size	4.030	1	1.20	-1.123	9.182
K-Substrate level	6.650	1	1.20	1.498	11.803
L-Incubation Temperature	-23.091	1	1.20	-28.243	-17.938

* Significant values, *df* : Degree of freedom, *P* : Level of significance

decreased and totally repressed by increasing the concentration up to 2%.

The optimum temperature for microbial enzyme production could be a function of the type of microorganism, composition, porosity, particle diameter and depth of the substrate and control of the fermentation process variables [34]. In the current study the optimal temperature for inulinase production of *Aspergillus sclerotiorum* Hoba2143 was 26°C, this result was in the similar mesophilic range of most fungi [47]. Ertan and Ekinci [13] found that the maximum inulinase activity of *Alternaria alternata* (2.3U/ml), *A. niger* (8.4 U/ml), and *Trichoderma harzanium* (1.2 U/ml) were obtained at 30, 35and 30°C respectively. Yu *et al.* [56] obtained maximum inulinase activity at low temperature

(28°C) by a mutant *Pichia guilliermondii*. Similarly, several temperature optima have been recorded for inulinase production, for example, 30°C for *A. fumigates* [17] and *Kluyveromyces marxianus* YS-1 [46], 28°C for *Penicillium citrinum* [44], 25°C for *Aspergillus wentii* [21] and 30°C for *Aspergillus niger* [18]. Increasing incubation temperature above its optima will gradually reduce the ability of microorganisms to secrete enzymes; this may be due to the denaturation of microbial strain at higher temperatures. Rising or decreasing incubation temperature away from the optimum will affect on the growth and enzymatic reaction rate inside the cells which consequently affect its potentiality to secrete microbial enzyme [28]

Selection of a suitable substrate for solid

Table 6. Central composite design matrix with the experimental and predicted values of inulinase production by *A. sclerotiorum* strain Hoba2143

| | Coded and natural values of independent variables | | | | Inulinase activity (Uml^{-1}) | | |
Run	Incubation temp. (°C)	NH$_4$ mixture (%)	Substrate level (g/flask)	Peptone (%)	Experimental	Predicted	Residual
1	0 (26)	-2 (0.7)	0 (1.25)	0 (0.6)	18.47	17.04	1.44
2	0 (26)	0 (1.3)	0 (1.25)	0 (0.6)	109.10	104.57	4.53
3	-1 (23)	1 (1.6)	1 (1.50)	-1 (0.5)	36.14	34.29	1.85
4	0 (26)	0 (1.3)	2 (1.75)	0 (0.6)	31.22	34.53	-3.31
5	1 (29)	1 (1.6)	-1 (1.00)	1 (0.7)	65.53	66.26	-0.73
6	1 (29)	-1 (1.0)	-1 (1.00)	-1 (0.5)	5.50	9.23	-3.73
7	0 (26)	0 (1.3)	0 (1.25)	0 (0.6)	105.12	104.57	0.55
8	0 (26)	0 (1.3)	0 (1.25)	2 (0.8)	39.45	40.94	-1.49
9	1 (29)	1 (1.6)	-1 (1.00)	-1 (0.5)	42.21	40.33	1.88
10	-1 (23)	1 (1.6)	-1 (1.00)	1 (0.7)	80.58	79.51	1.07
11	0 (26)	0 (1.3)	0 (1.25)	0 (0.6)	104.12	104.57	-0.45
12	0 (26)	0 (1.3)	0 (1.25)	0 (0.6)	101.10	104.57	-3.47
13	-1 (23)	-1 (1.0)	1 (1.50)	1 (0.7)	21.06	19.73	1.33
14	0 (26)	2 (1.9)	0 (1.25)	0 (0.6)	76.58	78.87	-2.29
15	2 (32)	0 (1.3)	0 (1.25)	0 (0.6)	10.83	12.06	-1.23
16	-1 (23)	1 (1.6)	1 (1.50)	1 (0.7)	51.83	50.46	1.37
17	1 (29)	-1 (1.0)	1 (1.50)	-1 (0.5)	28.17	26.02	2.15
18	1 (29)	1 (1.6)	1 (1.50)	-1 (0.5)	31.25	30.95	0.30
19	0 (26)	0 (1.3)	-2 (0.75)	0 (0.6)	49.25	46.79	2.46
20	0 (26)	0 (1.3)	0 (1.25)	0 (0.6)	103.00	104.57	-1.57
21	-1 (23)	-1 (1.0)	1 (1.50)	-1 (0.5)	18.31	19.94	-1.63
22	1 (29)	1 (1.6)	1 (1.50)	1 (0.7)	42.10	40.03	2.07
23	0 (26)	0 (1.3)	0 (1.25)	0 (0.6)	105.00	104.57	0.43
24	1 (29)	-1 (1.0)	-1 (1.00)	1 (0.7)	20.15	18.79	1.36
25	-1 (23)	-1 (1.0)	-1 (1.00)	-1 (0.5)	7.11	5.97	1.14
26	-2 (20)	0 (1.3)	0 (1.25)	0 (0.6)	19.61	19.23	0.38
27	-1 (23)	-1 (1.0)	-1 (1.00)	1 (0.7)	19.94	22.61	-2.67
28	1 (29)	-1 (1.0)	1 (1.50)	1 (0.7)	18.75	18.73	0.02
29	-1 (23)	1 (1.6)	-1 (1.00)	-1 (0.5)	44.11	46.50	-2.39
30	0 (26)	0 (1.3)	0 (1.25)	-2 (0.4)	15.86	15.22	0.64

state fermentation process is one of the most crucial factors, where substrate not only provides the nutrient for the microbial growth but also act as a support for microbial cells attachment [33]. Substrate particles size, level and moisture content are the most critical factors which influence the microbial growth and activity [41], due to their effect on microbial respiration and aeration. In this study maximum inulinase productivity (5721.5U/gm substrate) was obtained at substrate level of 1.2 g /250ml conical flask

Statistical optimization of fermentation process variables for inulinase production by *A. sclerotiorum* strain Hoba2143 using central composite design (CCD)

Results of Placket-Burman design revealed that, incubation temperature (X_1), NH_4 mixture (X_2), substrate level (X_3) and peptone (X_4) were the most significant independent variables affecting inulinase production, thus they were selected for further optimization using five level central composite design (CCD). Table 6 shows the four independent variables and their concentrations at different coded and actual levels of the variables employed in the design matrix. Other insignificant variables were set at their center points of PB design. Central composite design

matrix and responses (experimental and predicted inulinase activity) for the 30 runs of the design are presented in Table 6, which shows considerable variation in the amount of inulinase activity depending on the four independent variables.

Based on the experimental data obtained; inulinase activity ranged from 5.50 to 109.10 Uml[-1], the highest levels of inulinase production (based on the amount of enzyme activity) were obtained in runs 2, 7, 11, 12, 20 and 23 (center points) with values of 109.10, 105.12, 104.12, 101.10, 103 and 105 Uml[-1] respectively, where incubation temperature 26°C, NH_4 mixture 1.3%, substrate level 1.25g/flask and peptone 0.6% were used, while the minimum inulinase production was observed in run number 6 where incubation temperature 29°C, NH_4 mixture 1%, substrate level 1g/flask and peptone 0.5% were used.

The CCD experimental data obtained were submitted to statistical analysis using design expert 7.0, the fit summary results in Table 7, contributed to find an adequate type of response surface model. Since the aim of sequential model sum of squares is to select the highest order polynomial where the additional terms are significant and lack of fit tests select the models that have insignificant lack of fit, also the model summary statistics focus on the

Table 7. Fit summary for CCD experimental data

Sequential Model Sum of Squares Source	Sum of Squares	*df*	Mean Square	*F*-value	*P*-value Prob >*F*
Linear	7029.25	4	1757.31	1.61	0.2023
Two factors interaction (2FI)	1384.43	6	230.74	0.17	0.9819
Quadratic	25746.76	4	6436.69	817.52	< 0.0001*
Residual	68.97	7	9.85		
Lack of Fit Tests Source	Sum of Squares	*df*	Mean Square	*F*-value	*P*-value Prob >*F*
Linear	27213.57	20	1360.68	190.48	< 0.0001*
Two factors interaction (2FI)	25829.14	14	1844.94	258.28	< 0.0001*
Quadratic	82.38	10	8.24	1.15	0.4646
Pure Error	35.72	5	7.14		
Model Summary Statistics Source	Standard deviation	R-Squared	Adjusted R-Squared	Predicted R-Squared	PRESS
Linear	33.02	0.2051	0.0779	0.0403	32896.99
Two factors interaction (2FI)	36.90	0.2455	-0.1517	-0.2707	43559.28
Quadratic	2.81	0.9966	0.9933	0.9847	525.97

* Significant values, *df* : degree of freedom, PRESS: sum of squares of prediction error

models that have lower standard deviation and higher adjusted and predicted R-squared; quadratic model type was selected to be the proper model that fit the CCD of inulinase production by *A. sclerotiorum* strain Hoba2143, where fit summary results (Table 7) showed that, the quadratic model is a highly significant model with a very low probability value $[(P_{model} > F) < 0.0001]$, also lack of fit F-value 1.15 (the lack of fit is not significant, $P > F = 0.4646$), finally the model summary statistics of the quadratic model showed the smallest standard deviation of 2.81 and the largest adjusted and predicted R-squared of 0.9933 and 0.9847 respectively. After selection of the proper response surface model type, analysis of variance (ANOVA) was carried out as shown in Table 8. The coefficients of regression equation were calculated and the data (Table 9) was fitted to a second-order polynomial equation. The inulinase production (Y) by *A. sclerotiorum* strain Hoba2143 can be expressed in terms of the following regression equation:

$$Y_{(Inulinase\ yield)} = +104.57 - 1.79\,X_1 + 15.46\,X_2 - 3.07\,X_3 + 6.43\,X_4 - 2.36\,X_1X_2 + 0.71\,X_1X_3 - 1.77\,X_1X_4 - 6.54\,X_2X_3 + 4.10\,X_2X_4 - 4.21\,X_3X_4 - 22.23\,X_1^2 - 14.16\,X_2^2 - 15.98\,X_3^2 - 19.12\,X_4^2$$

$$Eq\,(4)$$

Where Y was the predicted response (value of inulinase yield Uml^{-1}), X_1, X_2, X_3 and X_4 were the coded levels of incubation temperature, NH_4 mixture, substrate level and peptone respectively.

The ANOVA of the quadratic regression model demonstrates that Equation (4) was a highly significant model, as was evident from the Fisher's F test (F value = 309.91) with a very low probability value $[P_{model} > F$ less than 0.0001] (Table 8). Values of "Prob > F" less than 0.05 indicate that model terms are significant. The significance in our model meant that there was only 0.01% chance that wrong prediction could occur due to experimental errors or noise factors. The high F-value and non significant lack of fit (P-value > F = 0.4646) also suggested that the obtained experimental data was a good fit with the model. The goodness of fit of the model was checked by determination coefficient (R^2); a value > 0.75 indicates good fitness of the model.

Studying the parameters from the ANOVA

statistical analysis (Table 8), showed that, by decomposing the model sum of squares into several sources, significant terms were verified based on their individual P values. In this study, our results revealed that, all linear (X_1, X_2, X_3 and X_4), quadric (X_1^2, X_2^2, X_3^2 and X_4^2) and interactive (X_1X_2, X_2X_3, X_2X_4 and X_3X_4) model terms had a very significant effect on inulinase production by *A. sclerotiorum* strain Hoba2143 with a probability of over 99%, except X_1X_4 (interaction between incubation temperature and peptone respectively) had a significant effect with a probability value of over 95% and X_1X_3 (interaction between incubation temperature and substrate level respectively) was the only insignificant model term, that not contribute to the response (inulinase production) at a significant level ($Prob > F = 0.3308) > 0.05$.

In this model the value of $R^2 = 0.9966$ (Table 8) indicated that, the model can explain 99.66% of response variations (99.66% of response variations was attributed to the independent variables) and only 0.34% of the total variations cannot explained by the model. In addition, the value of the adjusted determination coefficient (Adj $R^2 = 0.9933$) was also very high to advocate for a high significance of the model (Table 8). The 'predicted R^2' value of 0.9847 was in a reasonable agreement with the 'adjusted R^2' value. At the same time, a relatively lower value of the coefficient of variation (CV = 5.92%) indicates a better precision and reliability of the experiments carried out (Table 8). The adequate precision value of the present model was 49.697 and this also suggests that the model can be used to navigate the design space. The adequate precision value is an index of the signal-to-noise ratio, and values of higher than 4 are essential prerequisites for a model to be a good fit.

The positive coefficients for X_2 (NH_4 mixture) and X_4 (peptone), 15.46 and 6.43 respectively (Table 9) indicate a linear effect to increase inulinase production, while negative coefficients for X_1 (incubation temperature) and X_3 (substrate level), -1.79 and -3.07 indicate a linear effect to decrease inulinase production.

Contour and three dimensional (3D) plots

The graphical representation (3D plot and its corresponding contour plot) provides a method for visualizing the relationship between the response and the interactions among test variables

Table 8. Regression statistics and analysis of variance (ANOVA) for
CCD results used for optimizing inulinase production by *A. sclerotiorum* strain Hoba2143

Source	Sum of Squares	df	Mean Square	F-value	P-value Prob >F
Model	34160.44	14	2440.03	309.91	< 0.0001*
X_1 - (Incubation temp.)	76.97	1	76.97	9.78	0.0069*
X_2 - (NH_4 mixture)	5734.42	1	5734.42	728.33	< 0.0001*
X_3 - (Substrate level)	225.58	1	225.58	28.65	< 0.0001*
X_4 - (Peptone)	992.28	1	992.28	126.03	< 0.0001*
$X_1 X_2$	88.92	1	88.92	11.29	0.0043*
$X_1 X_3$	7.95	1	7.95	1.01	0.3308
$X_1 X_4$	50.2	1	50.2	6.38	0.0233*
$X_2 X_3$	685.13	1	685.13	87.02	< 0.0001*
$X_2 X_4$	268.3	1	268.3	34.08	< 0.0001*
$X_3 X_4$	283.92	1	283.92	36.06	< 0.0001*
X_1^2	13557	1	13557	1721.87	< 0.0001*
X_2^2	5496.35	1	5496.35	698.09	< 0.0001*
X_3^2	7002.71	1	7002.71	889.41	< 0.0001*
X_4^2	10030.68	1	10030.68	1273.99	< 0.0001*
Residual	118.1	15	7.87		
Lack of Fit	82.38	10	8.24	1.15	0.4646
Pure Error	35.72	5	7.14		
Cor Total	34278.54	29			
Std. Dev.	2.81	R-Squared	0.9966		
Mean	47.38	Adj R-Squared	0.9933		
C.V. %	5.92	Pred R-Squared	0.9847		
PRESS	525.97	Adeq Precision	49.697		

* Significant values, *df* : Degree of freedom, *F*: Fishers's function, *P* : Level of significanceC.V: Coefficient of variation

Table 9. Regression coefficients of second order polynomial model for optimization of
inulinase production by *A. sclerotiorum* strain Hoba2143

| Factor	Coefficient estimate	Standard error	95% CI Low	95% CI High
Intercept	104.57	1.15	102.13	107.01
X_1 - (Incubation temp.)	-1.79	0.57	-3.01	-0.57
X_2 - (NH_4 mixture)	15.46	0.57	14.24	16.68
X_3 - (Substrate level)	-3.07	0.57	-4.29	-1.85
X_4 - (Peptone)	6.43	0.57	5.21	7.65
$X_1 X_2$	-2.36	0.70	-3.85	-0.86
$X_1 X_3$	0.71	0.70	-0.79	2.2
$X_1 X_4$	-1.77	0.70	-3.27	-0.28
$X_2 X_3$	-6.54	0.70	-8.04	-5.05
$X_2 X_4$	4.10	0.70	2.6	5.59
$X_3 X_4$	-4.21	0.70	-5.71	-2.72
X_1^2	-22.23	0.54	-23.37	-21.09
X_2^2	-14.16	0.54	-15.3	-13.01
X_3^2	-15.98	0.54	-17.12	-14.84
X_4^2	-19.12	0.54	-20.27	-17.98

in order to determine the optimum conditions for inulinase production. 3D plots for the significant pair-wise combinations of the four variables (X_1 X_2, $X_1 X_4$, $X_2 X_3$, $X_2 X_4$ and $X_3 X_4$) were generated by plotting the response (inulinase yield) on Z-axis against two independent variables while keeping the other variables at their center points (zero levels).

The 3D plot and its corresponding contour plot (Fig. 6A), showing the effects of incubation temperature (X_1) and NH_4 mixture concentration (X_2) on inulinase production, while substrate level (X_3) and peptone concentration (X_4) were kept at their zero levels (1.25 gflask^{-1} and 0.6%) respectively. It can be seen that, when the incubation temperature approximate to 26°C, the yield of inulinase increases gradually by increasing NH_4 mixture concentration, but decreases beyond NH_4 mixture high concentration. Beyond 26°C, inulinase yield decreases (negative effect) and the effect of NH_4 mixture concentration on inulinase yield was not significant. By solving the inverse matrix (Equation 4) using the Design-Expert Software and analysis of Fig. 6A, the maximum predicted inulinase yield of 108.9 U.ml^{-1} was obtained at the optimum predicted levels of incubation temperature and NH_4 mixture concentration of 25.79°C and 1.47% respectively. 3D plot and its corresponding contour plot (Fig. 6B), describes the effects of incubation temperature (X_1) and peptone concentration (X_4) on inulinase production, when substrate level (X_3) and NH_4 mixture concentration (X_2) were kept at their zero levels (1.25 gflask^{-1} and 0.1.3%) respectively. It is evidence that the yield of inulinase production steadily increased at low degrees of incubation temperature when peptone concentration increased till reach its optimum concentration after which inulinase yield decreased. At high temperatures beyond 26°C inulinase yield decreased and the effect of peptone concentration on inulinase yield was not significant. By solving the inverse matrix (Equation 4) and analysis of Fig. 6B, the maximum predicted inulinase yield of 105.16 U.ml^{-1} was obtained at the optimum predicted levels of incubation temperature and peptone concentration of 25.86°C and 0.62% respectively. 3D plot and its corresponding contour plot (Fig. 6C), highlight the roles played by NH_4 mixture concentration (X_2) and substrate level (X_3) on

inulinase production when incubation temperature (X_1) and peptone concentration (X_4), were kept at their zero levels (26°C and 0.6%) respectively. Analysis of Fig. 6C clearly suggests that as substrate level increased, increase in inulinase yield occurred with increasing NH_4 mixture concentration, but further increase in substrate level above 1.2 gflask^{-1} leads to decrease in inulinase yield. At low levels of NH_4 mixture concentration, the effect of substrate level on inulinase yield was not significant. By solving the inverse matrix (Equation 4) and analysis of Fig. 6C, the maximum predicted inulinase yield of 109.48 U.ml^{-1} was obtained at the optimum predicted levels of NH_4 mixture concentration and substrate level of 1.49% and 1.2 gflask^{-1} respectively. 3D plot and its corresponding contour plot (Fig. 6D), highlight the roles played by NH_4 mixture concentration (X_2) and peptone concentration (X_4) on inulinase production when incubation temperature (X_1) and substrate level (X_3), were kept at their zero levels (26°C and 1.25 gflask^{-1}) respectively. As the value of independent variables (NH_4 mixture and peptone concentrations) increased, the yield of inulinase increased gradually but only up to the optimum levels of the independent variables and thereafter the yield decreased even though the values of the variables increased. By solving the inverse matrix (Equation 4) and analysis of Fig. 6D, the maximum predicted inulinase yield of 109.76 U.ml^{-1} was obtained at the optimum predicted levels of NH_4 mixture and peptone concentrations of 1.48% and 0.62% respectively.

The interactive effect of substrate level (X_3) and peptone concentration (X_4) on inulinase production when incubation temperature (X_1) and NH_4 mixture concentration (X_2), were kept at their zero levels (26°C and 1.3%) respectively is depicted in Fig. 6E. When substrate level increased from 1 to around 1.25 g flask^{-1}, an increase in inulinase yield from 68.9 to 104.6 U.ml^{-1} occurred with increasing peptone concentration. Increasing substrate level beyond 1.25 g flask^{-1} decreases inulinase yield (negative effect) at high or low levels of peptone concentration. The maximum predicted inulinase yield of 105.34 U.ml^{-1} was obtained at the optimum predicted levels of substrate level and peptone concentrations of 1.22 g flask^{-1} and 0.62% respectively. The maximum
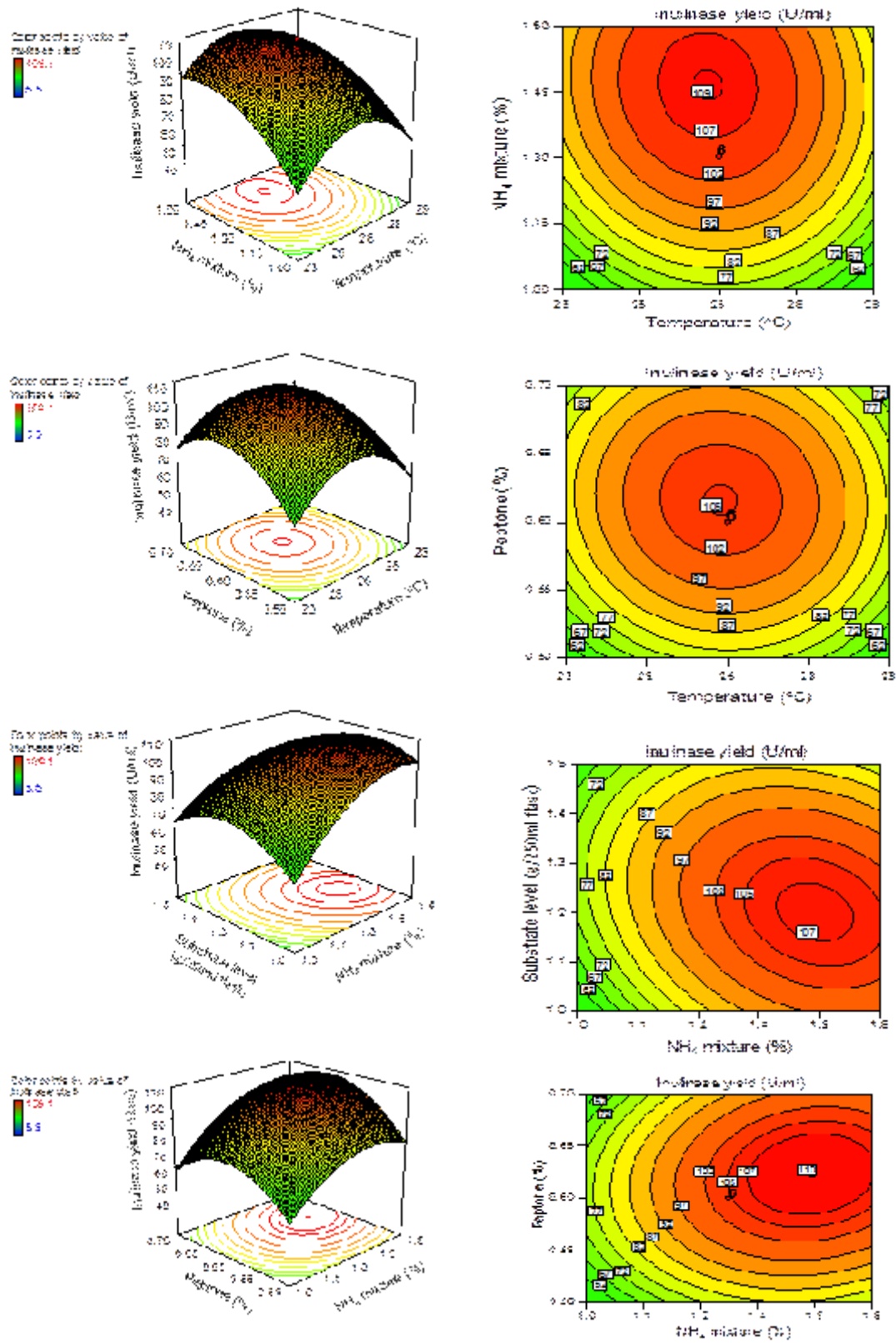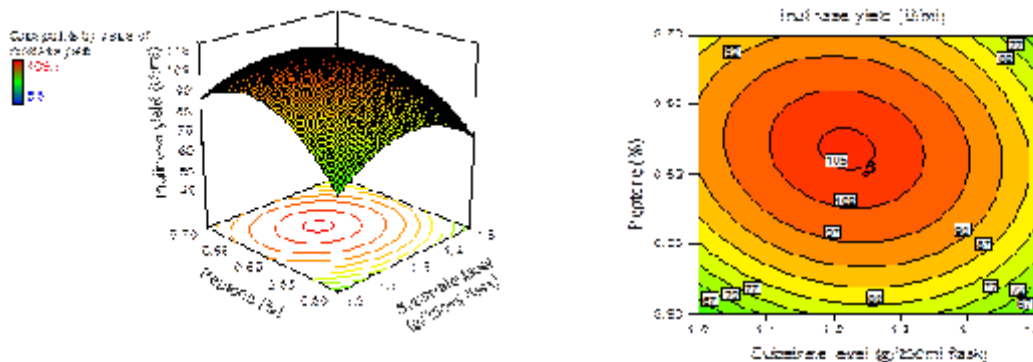
Fig.6. 3D response surface and contour plots of the effects of NH_4 mixture concentration, peptone concentrations, substrate level and incubation temperature on inulinase production by *A. sclerotiorum* strain Hoba2143

experimental value of inulinase yield of 104.57 U.ml^{-1} was obtained at the center points (zero-levels) of the investigated independent variables (incubation temperature 26°C, NH_4 mixture concentration 1.3%, substrate level 1.25 g flask^{-1} and peptone concentration of 0.6%).

Model adequacy checking

Usually, it is necessary to check the fitted model to ensure that it provides an adequate approximation to the real system. Unless the model shows an adequate fit, proceeding with the investigation and optimization of the fitted response surface likely give poor or misleading results. Checking of adequacy of the model needs all of the information on lack of fit, which is contained in the residuals.

The normal probability plot is an important diagnostic tool that indicates whether the residuals follow a normal distribution (normality assumption), in which case the points will follow a straight line expect some scatter even with normal data. Fig. 7A showed that, the normality assumption was satisfied as the residual plot approximated a long a straight line for inulinase production, this indicates that the model was well fitted with the experimental results. As the residuals from the fitted model were normally distributed, all the major assumptions of the model had been validated. Fig. 7B presents a plot of residuals versus the predicted response. The plot showed that the residuals scatter randomly on the display, suggesting that the variance of the original observation is constant for all values of inulinase yield. Thus, the plot of inulinase production was satisfactory; this

indicated that the model is adequate to describe the inulinase activity by response surface. Also, predicted versus actual inulinase yield plot as a visual diagnostic plot indicated that, there is a close agreement between the experimental results and theoretical values predicted by the model equation as shown in Fig. 7C, which confirms the adequacy of the model.

Box–Cox plot provides guideline for selecting the correct power law transformation to further improve the model. As observed from Fig. 7D, the blue line indicates the current transformation (Lambda = 1) and the green line indicates the best lambda value (Lambda = 1.06), while the red lines indicate the minimum and maximum 95% confidence interval values (0.83 and 1.3 respectively). Therefore, the model needs no transformation, as current value of confidence interval ($\lambda = 1$) is very close to model design value (best = 1.06) and the model is in the optimal zone since the blue line falls within the red lines. So that the model is well fit to the experimental data obtained and well satisfies the assumptions of the analysis of variance.

Validation of the model

In order to determine accuracy of the model and to verify the optimization results, experiments were repeated in triplicates under optimized culture conditions obtained from fitted inulinase production model i.e. 26°C of incubation temperature, 1.54% of NH_4 mixture, 1.20 g flask^{-1} of substrate level and 0.64% peptone. Under these conditions, 114.43±1.35 Uml^{-1} of inulinase activity was obtained. This value of inulinase activity

corresponds very well to the values predicted by the fitted model 110.06 Uml^{-1}.

Finally, after initial survey using "Jerusalem artichoke + bagasse" as a substrate for screening inulinolytic potentialities of microorganisms (step1), classical optimization by one factor at a time for different agriculture residues and fermentation period (step 2), statistical optimization by Plackett-Burman design (step 3), central composite design (step 4) and validation under optimized conditions (step 5), it was found that, inulinase yield of *A. sclerotiorum* strain Hoba2143 was increased from 10.7 to 114.43 Uml^{-1}. With a fold of increase 2.7, 7.9, 9.77 and 10.69

respectively. The maximum inulinase yield of 114.43 Uml^{-1} is equivalent to 5721.5 Ugds^{-1}; as batch fermentation contents were eluted in 50 ml buffer solution.

Inulin hydrolysis by partially purified inulinase

TLC procedure was carried out to separate hydrolysis by-products of inulin, this enables us to characterize the mode of action of the enzyme and particularly, if it is of the endo-or exo- type. Partially purified inulinase was incubated with 1% inulin solution for different incubation periods, the enzyme hydrolyzate loaded into TLC aluminum sheets, the hydrolysis products were visualized by aniline-diphenylamine reagent.
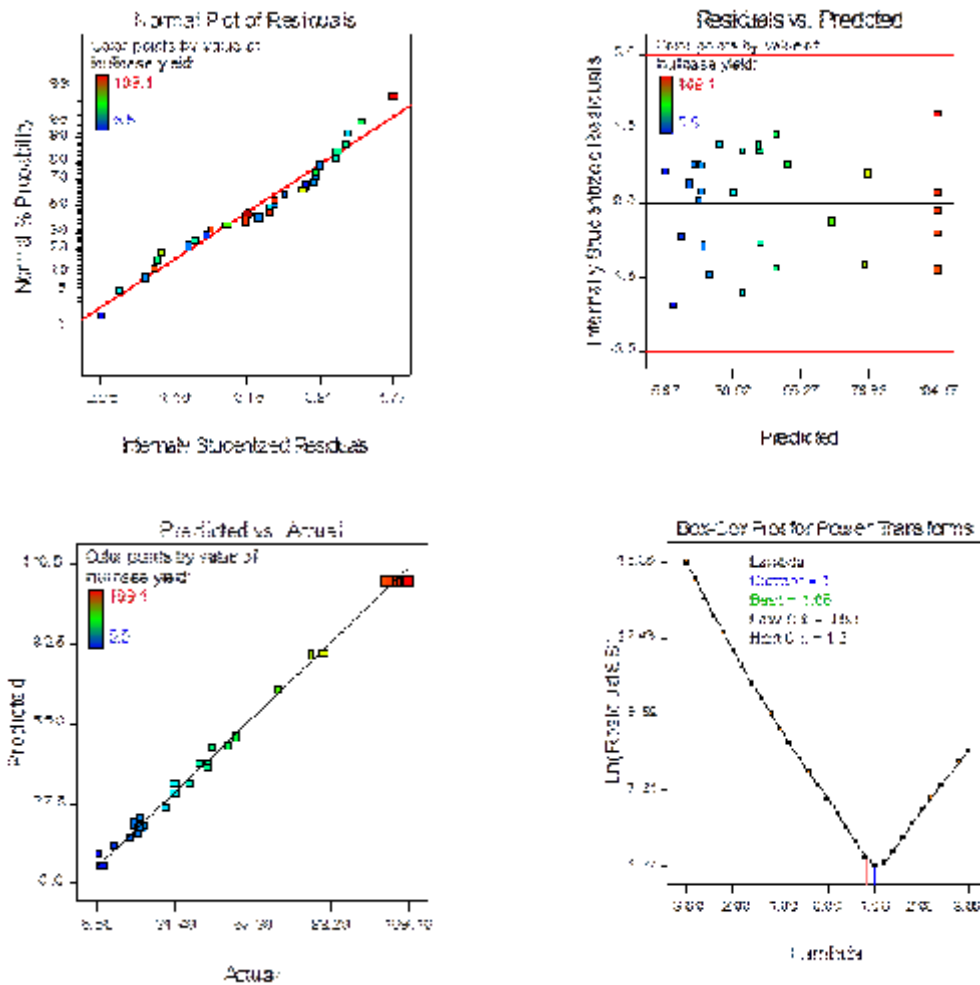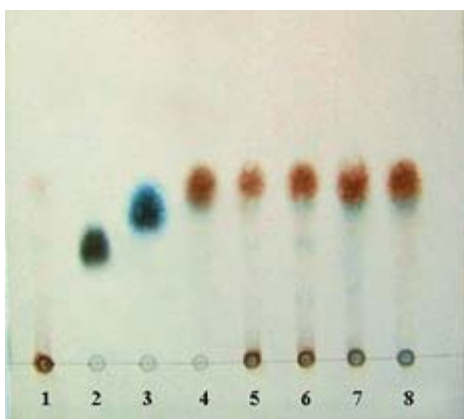

Fig. 7. (A) Normal probability plot of internally studentized residuals, (B) plot of internally studentized residuals versus predicted inulinase yield, (C) plot of predicted versus actual inulinase yield by *A. sclerotiorum* strain Hoba2143 using CCD and (D) Box- Cox plot of model transformation.

Chromatogram (Fig. 8) indicated that fructose produced early in the hydrolysis of inulin after 5 min incubation.

Inulinases are usually inducible and classified into exo- and endo-inulinases according to their mode of action on inulin [30]. Exo-inulinases (β-D-fructan fructohydrolase, EC 3.2.1.80) split terminal fructose units successively from the non-reducing end of inulin to liberate fructose. The exo-acting inulinases hydrolyze sucrose and the fructose portion of raffinose in addition to inulin [32]. In contrast, endo-inulinases (2, 1- β-D-fructan fructanohydrolase, EC 3.2.1.7) are specific for inulin and hydrolyze the internal β-(2→1)-fructofuranosidic linkages that are located away from the ends of the polymer network to yield inulotriose, inulotetrose and inulopentose as the main products [8]. In the present work, inulin hydrolysis occurred early after 5 min of incubation. Analysis of the inulin hydrolysis products by TLC showed the release of fructose as an end product (Fig. 8). Release of fructose as an end product of inulin hydrolysis and no fructose oligomers are detected; therefore it is clear that *A. sclerotiorum* Hoba2143 inulinase is an exo-type. Fructose is generally recognized as safe alternative sweetener to sucrose because it has beneficial effects in diabetic patients, increases the iron absorption in children, used as a low calorie sweetener, highly soluble and, has low viscosity and higher sweetening capacity [34]. These physiological advantages allow fructose utilization as a sugar substitute in food and pharmaceutical preparations. Thus, production of ultra high fructose syrup from inulin has received a great industrial interest [57].

CONCLUSION

The present work demonstrates the production of inulinase by a newly isolated fungal strain *A. sclerotiorum* Hoba2143 on low cost substrates of rice straw and Jerusalem artichoke tuber under SSF. The applicability of statistical approach proved useful for the optimization of culture conditions for inulinase production. The maximum yield of inulinase achieved was 114.43 Uml^{-1} (5721.5 $Ugds^{-1}$); which was the highest yield reported so far.

REFERENCES

1. Azhari, R., Szlak, A.M., Ilan, E., Sideman, S., Lotan, N. Purification and characterization of endo- and exo-inulinase. *Biotechnol. Appl. Biochem.,* 1989; **11**: 105-117.
2. Baldrian, P., Gabriel, J. Lignocellulose degradation by *Pleurotus ostreatus* in the presence of cadmium. *FEMS Microbiol. Lett.,* 2003; **220**: 235-240.
3. Bradford, M. M. A rapid and sensitive method for the quantitation of microgram quantities of protein utilizing the principle of protein-dye binding. *Anal. Biochem.*, 1976; **72**: 248-254.
4. Castilho, L. R., Medronho, R. A., Alves, T. L. Production and extraction of pectinases obtained by solid state fermentation of agroindustrial residues with *Aspergillus niger. Bioresour. Technol.*, 2000; **71**: 45-50.
5. Chakravarti R., Sahai V. Optimization of compactin production in chemically defined production medium by *Penicillium citrinum* using statistical methods. *Process Biochem.*, 2002; **38**: 481-486.
6. Chen, H.-Q., Chen, X.-M., Chen, T.-X., Xu, X.-M. , Jin, Z.-Y. Extraction optimization of inulinase obtained by solid state fermentation of *Aspergillus ficuum* JNSP5-06. *Carbohydr. Polym.*, 2011; **85**: 446-451.
7. Chen, X., Wang, J., Li, D. Optimization of solid-state medium for the production of inulinase by *Kluyveromyces* S120 using response surface methodology. *Biochem. Eng. J.*, 2007; **34**: 179–184.

Fig. 8. Thin layer chromatogram for hydrolysis by-products of inulin by partially purified *A. sclerotiorum* Hoba 2143 inulinase. Lane 1: control (inulin + boiled inulinase), 2: sucrose, 3: glucose, 4: fructose (as standards), 5, 6, 7 and 8 are hydrolysis products after 5, 10, 15 and 30 min incubation, respectively.

8.   Chi, Z.M., Zhang, T., Cao, T.S., Liu, X.Y., Cui, W., Zhao, C.H. Biotechnological potential of inulin for bioprocesses. *Biores. Technol.,* 2011; **102**: 4295-4303.

9.   Derycke, D.G., Vandamme, E.J. Production and properties of *Aspergillus niger* inulinase . *J. Chem. Tech. Biotechnol.*, 1984; **34**: 45-51.

10.   Dinarvand, M., Ariff, A.B., Moeini, H., Masomian, M., Mousavi, S.S., Nahavandi, R., Mustafa, S. Effect of extrinsic and intrinsic parameters on inulinase production by *Aspergillus niger* ATCC 20611. *Electronic J. Biotechnol.*, 2012; ISSN: 0717-3458.

11.   Domsch, K., Gams, W., Anderson, T. Compendium of Soil Fungi. 1, 1264., IHW-Verlag, Germany, 1993; ISBN: 9783980308380.

12.   El-Hersh, M. S., Saber, W. I., El-Naggar, N.E. Production strategy of inulinase by *Penicillium citrinum* AR-IN2 on some agricultural by-products. *Microbiol. J.*, 2011; **1**: 79-88.

13.   Ertan F, Ekinci F. The production of inulinases from *Alternaria alternata*, *Aspergillus niger* and *Trichoderma harzianum*. *J. Marmara Pure Appl. Sci.*, 2002; **18**: 7-15.

14.   Felsenstein, J. Confidence limits on phylogenies: an approach using the bootstrap. *Evolution.*, 1985; **39**: 783-791.

15.   Gao, H., Liu, M., Liu, J., Dai, H., Zhou, X., Liu, X., Zhuo, Y., Zhang, W. and Zhang, L. Medium optimization for the production of avermectin B1a by *Streptomyces avermitilis* 14-12A using response surface methodology. *Bioresour. Technol.*, 2009; **100**: 4012-4016.

16.   Gill, P. K., Sharma, A. D., Harchand, R. K., Singh, P. Effect of media supplements and culture conditions on inulinase production by an actinomycete strain. *Bioresour. Technol.*, 2003; **87**: 359-362.

17.   Gouda, M.K. Some properties of inulinase from *Aspergillus fumigatus*. *Pakistan J. Biol. Sci.*, 2002; **5**: 589-593.

18.   Housseiny, M.M. Production of an endoinulinase from *Aspergillus niger* AUMC 9375 by solid state fermentation of agricultural wastes, with purification and characterization of the free and immobilized enzyme. *J. Microbiol.*, 2014; **52**: 389-398.

19.   Inglis, P.W., Tigano, M.S. Identification and taxonomy of some entomopathogenic *Paecilomyces* spp. (Ascomycota) isolates using rDNA-ITS Sequences. *Gen. Mol. Biol.*, 2006; **29**: 132-136.

20.   Jing, W., Zhengyu, J., Bo, J., Augustine, A. Production and separation of exo- and endoinulinase from *Aspergillus ficuum*. *Process Biochem.*, 2003; **39**: 5-11.

21.   Karatop, R., Sanal, F. A. A potential resource in fructose production from inulin: *Aspergillus wentii* inulinase. *J. Cell. Mol. Biol.*, 2013; **11**: 21-28.

22.   Kaur, A., Sharma, D., Harchand, R.K., Singh, P., Bhullar, S.S., Kaur, A. Production of a thermostable extracellular inulinase by *Aspergillus fumigatus*. *Indian J. Microbiol.*, 1999; **39**: 99-103.

23.   Kochhar, A., Kaur, N., Gupta, A.K. Inulinase from *Aspergilus versicolor*: A potent enzyme for fructose from inulin. *J. Sci. Ind. Res.*, 1997; **56**: 721-726.

24.   Kumar, G. P., Kunamneni, A., Prabhakar, T. Optimization of process parameters for the production of inulinase from a newly isolated *Aspergillus niger* AUP19. *World J. Microbiol. Biotechnol.*, 2005; 21: 1359-1361.

25.   Li, A. X., Guo, L. Z., Fu, Q., Lu, W. D. A simple and rapid plate assay for screening of inulin degrading microorganisms using Lugol's iodine solution. *Afr. J. Biotechnol.*, 2011; **46**: 9518-9521.

26.   Li, A.X. Guo, L.Z. Lu, W.D. Alkaline inulinase production by a newly isolated bacterium *Marinimicrobium* sp. LS-A18 and inulin hydrolysis by the enzyme. *World. J. Microbiol. Biotechnol.*, 2012; **28**: 81-89.

27.   Mahmoud, D.A.R., Mahdy, E.M.E., Shousha, W.G., Refaat,. H.W., Abdel-Fattah, A.F. Raw garlic as a gew substrate for inulinase production in comparison to dry garlic. *Australian J .Basic Appl. Sci*., 2011; **5**: 453-462.

28.   Moat, A.G., Foster, J.W., Spector, M.P. Microbial physiology. 4th ed. Wiley-Liss, Inc., New York. 2002; 1:1-28.

29.   Montgomery, D.C. Design and analysis of experiments: Response surface methods and designs. NewJersey: John Wiley and Sons, Inc., 2005; **210**: 56.

30.   Nakamura, T., Shady, S.M., Nakatsu, S. Action and production of inulinase. *Denpun Kagaku.*, 1988; **35**: 121-130.

31.   Nakamura, T., Shitara, A., Matsuda, S., Matsuo, T., Suiko, M., Ohta, K. Production, purification and properties of an endoinulinase of *Penicillium* sp. TN-88 that liberates inulotriose. *J. Ferment. Bioeng.*, 1997; **84**: 313-318.

32.   Ohta, K., Norio, N., Nakamura, T. Purification and properties of an extracellular inulinases from *Rhizopus* sp. strain TN–96. *J Biosci Bioeng.*, 2002; **94**: 78–80.

33.   Pandey, A., Soccol, C. R., Mitchell, D. New developments in solid state fermentation: I-bioprocesses and products. *Process Biochem.*, 2000; **35**: 1153-1169.

34. Pandey, A., Soccol, C. R., Selvakumar, P., Soccol, V. T., Krieger, N., Fontana, J. D. Recent developments in microbial inulinases: its production, properties and industrial applications. *Appl. Biochem. Biotechnol.*, 1999; **81**: 35-52.

35. Plackett, R.L., Burman, J.P. The design of optimum multifactorial experiments. *Biometrika*, 1946; **33**: 305-325.

36. Reddy, P. R. M., Ramesh, B., Mrudula, S., Reddy, G., Seenayya, G. Production of thermostable â-amylase by *Clostridium thermosulfurogenes* SV2 in solid-state fermentation: Optimization of nutrient levels using response surface methodology. *Process Biochem.*, 2003; **39**: 267-277.

37. Saber, W.A. , El-Naggar, N.E. Optimization of fermentation conditions for the biosynthesis of inulinase by the new source; *Aspergillus tamarii* and hydrolysis of some inulin containing agro-wastes. *Biotechnol.*, 2009; **8**: 425-433.

38. Saitou, N., Nei, M. The neighbor-joining method: a new method for reconstructing phylogenetic trees. *Mol. Biol. Evol.*, 1987; **4**: 406-425.

39. Samson, R.A. Current taxonomic schemes of the genus *Aspergillus* and its teleomorphs. In: *Aspergillus*: The Biology and Industerial Applications, Bennett, J.W. and M.A. Klich (Eds.). Butterworth-Heinemann, USA., ISBN: 9780750691246, 1992; pp: 353-388.

40. Sanal F.E., Ertan F., Aktac T. Production of exo-inulinase from *Alternaria alternata* grown on Jerusalem artichoke and some biochemical properties. *J. Biol. Sci.*, 2005; **5**: 497-505.

41. Sarrette, M., Nout, M. J. R., Gervais, P., Rombouts, F. M. Effect of water activity on production and activity of *Rhizopus oligosporus* polysaccharides. *Appl. Microbiol. Biotechnol.*, 1992; **37**: 420-425.

42. Selvakumar, P., Pandey, A. Comparative studies on inulinase synthesis by *Staphylococcus* sp. and *Kluyveromyces marxianus* in submerged culture. *Bioresour. Technol.*, 1999; **94**: 123–127.

43. Sette, L., Passarini, M., Delarmelina, C., Salati, F., Duarte, M. Molecular characterization and antimicrobial activity of endophytic fungi from coffee plants. *World J. Microbiol. Biotechnol.*, 2006; **22**: 1185-1195.

44. Shady, T.S.M., Hauka, F.I.A., El-Sawah, M.M.A. Inulin hydrolysis by *Kluyveromyces marxianus* inulase produced on some agricultural wastes. *Egypt J. Microbiol.*, 2000; **35**: 139-154.

45. Sharma A. D., Kainth S., Gill P. K. Inulinase production using garlic (*Allium sativum*) powder as a potential substrate in *Streptomyces* sp. *J. Food Eng.*, 2006; **77,** 486-491.

46. Singh, P., Gill, P. Production of inulinases: Recent advances. *Food Technol. Biotechnol.*, 2006; **44(2)**: 151-162.

47. Singh, R. S., Singh, R. P. Production of fructo-oligosaccharides from inulin by endoinulinases, their prebiotic potential. *Food Technol. Biotechnol.*, 2010; **48**: 435–450.

48. Singh, R. S., Sooch, B. S., Puri, M. Optimization of medium and process parameters for the production of inulinase from a newly isolated *Kluyveromyces marxianus* YS-1. *Bioresour. Technol.*, 2007; **98**: 2518-2525.

49. Singhania, R. R., Patel, A. K., Soccol, C. R., Pandey, A. Recent advances in solid-state fermentation. *Biochem. Eng. J.*, 2009; **44**: 13-18.

50. Somogyi, M. Notes on sugar determination. *J. Biol. Chem.*, 1952; **195**: 19-23.

51. Tamura, K., Dudley, J., Nei, M., Kumar, S. MEGA4: Molecular Evolutionary Genetics Analysis (MEGA) software version 4.0. *Mol. Biol. Evol.*, 2007; **24**: 1596-1599.

52. Toyohiko, N., Akichika, S., Shusaku, M. Production, purification and properties of an endoinulinase of *Penicillium* sp. TN-88 that liberates inulotriose. *J. Ferment. Bioen.*, 1997; **84**: 313-318.

53. Vandamme, E. J., Derycke, D. G. Microbial inulinases: fermentation process, properties, and applications. *Adv. Appl. Microbiol.*, 1983; **29**: 139-176.

54. Warcup, J. H. The soil-plate method for isolation of fungi from soil. *Nature,* 1950; **166**: 117-118.

55. Xiong, C., Jinhua, W., Dongsheng, L. Optimization of solid-state medium for the production of inulinase by *Kluyveromyces* S120 using response surface methodology. *Biochem. Eng. J.*, 2007; **34**: 179-184.

56. Yu, X., Guo, N., Chi, Z., Gong, F., Sheng, J.,Chi, Z. Inulinase overproduction by a mutant of the marine yeast *Pichia guilliermondii* using surface response methodology and inulin hydrolysis. *Biochem. Eng. J.*, 2009; **43**: 266-271.

57. Zhang, L., Wang, Y. Gene engineering of producing fructose by inulase hydrolyzing *Helianthus tuberosus*. Chinese Patent 1465699, 2004.